ACS Catalysis

Research Article

pubs.acs.org/acscatalysis

In Situ-DRIFTS Study of Selective Catalytic Reduction of NO_x by NH_3 over Cu-Exchanged SAPO-34

Di Wang,[†] Li Zhang,[†] Krishna Kamasamudram,[‡] and William S. Epling*[,†]

[†]Department of Chemical and Biomolecular Engineering, University of Houston, 4800 Calhoun Road, Houston, Texas 77204-4004, United States

[‡]Cummins Inc., 1900 McKinley Avenue, Columbus, Indiana 47201, United States

Supporting Information

ABSTRACT: The intrinsic mechanism of the selective catalytic reduction (SCR) reaction over a Cu-exchanged SAPO-34 catalyst at low temperature was studied by in situ diffuse reflectance infrared Fourier transform spectroscopy (DRIFTS), coupled with mass spectrometry to measure inlet and outlet gas concentrations. The evolution of the surface intermediates, as well as the reactivity of NH_3 with surface NO_x species and NO_x with surface NH_3 species, was evaluated. In terms of NO_x adsorption, surface nitrates and nitrites are the main NO_x adsorption species at low temperature. When NO was exposed to the sample with NH_3 preadsorbed, surface NH_3 was not reactive because of the low surface coverage of nitrates and nitrites. However, the reactivity is significantly enhanced by the inclusion of O_2 in the feed, which promotes an increase in the concentration of surface nitrates and nitrites. DRIFTS results also reveal that the low temperature SCR reaction involves the formation of an NH_4NO_3 intermediate and its subsequent reduction by NO. The NH_4NO_3 was formed on Lewis acid sites on the Cu-SAPO-34 sample. The Brønsted acid sites act as an NH_3 reservoir that supplies additional NH_3 via migration to the Lewis acid sites for the SCR reaction. The migration of NH_3 between different acid sites was confirmed in an NH_3-temperature-programmed desorption (TPD) study. The presence of NO in the feed reduces surface NH_4NO_3 to produce N_2 at temperatures as low as 100 °C. Since NH_4NO_3 is typically considered an inhibitor, the onset temperature of the reaction between NO and NH_4NO_3 is much lower than that reported for other SCR zeolite catalysts; therefore, it is likely the key factor that results in the low temperature SCR activity of Cu-SAPO-34.

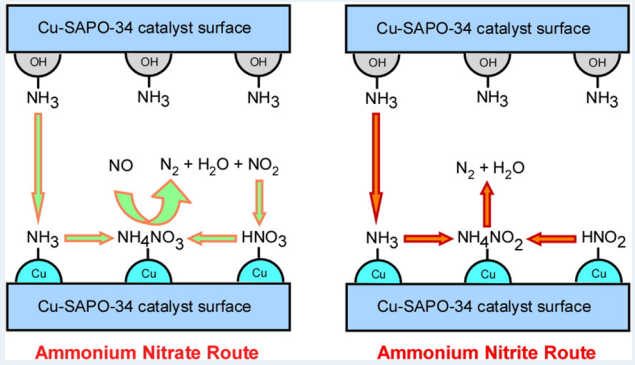

KEYWORDS: *selective catalytic reduction, SAPO-34, NO_x reduction, in situ DRIFTS*

1. INTRODUCTION

Nitrogen oxides, NO_x (NO + NO_2), are considered significant air pollutants. Selective catalytic reduction (SDR) of NO_x with NH_3 (NH_3−SCR) is a leading technology candidate for NO_x emissions control for diesel engine vehicles.[1] In general, NH_3−SCR includes three main reactions depending on the NO_2/NO_x ratio in the feed. Since NO is the major NO_x component (>90%) in the exhaust, the reaction between NO and NH_3 is the so-called "standard SCR" reaction:

$$4NH_3 + 4NO + O_2 \rightarrow 4N_2 + 6H_2O$$

If NO and NO_2 are in equimolar concentrations in the feed, the overall SCR reaction rate is increased and the "fast SCR" reaction occurs:

$$2NH_3 + NO + NO_2 \rightarrow 2N_2 + 3H_2O$$

If the fraction of NO_2 is larger than NO, a reaction between NO_2 and NH_3 can occur, termed "slow SCR" " or "NO_2−SCR":

$$4NH_3 + 3NO_2 \rightarrow 3.5N_2 + 6H_2O$$

In stationary applications, vanadia-based NH_3−SCR catalyst are used. However, these suffer from low activity and selectivity at high temperature. Other drawbacks are oxidation of SO_2 to SO_3, the formation of N_2O, and the toxicity of vanadia if it sublimes at high temperature.[2] Since first discovered by Iwamoto et al., transition metal exchanged zeolite frameworks with medium and large pores, such as MFI (ZSM-5), FER, and BEA, have been considered SCR catalysts candidates.[3] Although there is still some argument, the roles of the transition metals (Fe or Cu) include promoting the NO oxidation reaction as well as creating acid sites for NH_3 adsorption.[4−6] In terms of the reaction mechanism, most agree that the Langmuir−Hinshelwood mechanism occurs, in which the reaction between adsorbed NH_3 and surface nitrites and nitrates are the key steps in NH_3−SCR of NO_x.[7−10] This reaction pathway includes (i) the formation of the surface nitrites and nitrates, (ii) the reduction of nitrates by NO to

Received: December 26, 2012
Revised: March 10, 2013
Published: March 26, 2013

form nitrites, (iii) the reaction between adsorbed NH_3 and nitrites to produce N_2 via ammonium nitrite decomposition, and (iv) the reaction between adsorbed NH_3 and nitrates to form ammonium nitrate and its subsequent reduction and/or decomposition to N_2 and N_2O. Alternatively, the Eley−Rideal mechanism has been proposed, where gas-phase NO_2 reacts with two adjacent NH_4^+ ions to form an $(NH_4)_xNO_2$ complex which can be further reduced to N_2 by NO.[5,11,12]

As mentioned above, early research showed zeolite-based catalysts with medium and large pore sizes resulted in good SCR activity. However, their hydrothermal instability was problematic. Recently, the Cu-exchanged chabazite framework type zeolite with small pore sizes, such as SAPO-34 and SSZ-13, has received a great deal of attention because of exceptional hydrothermal durability and enhanced SCR activity, which has enabled its commercial introduction for on-highway diesel applications.[13−16] Lobo et al.[13] reported that the better SCR performance of Cu-CHA was due to the location of active Cu ions in the double six-membered rings (d6r). Beale et al.[17] confirmed the location of Cu atoms in the d6r unit and found that isolated mononuclear Cu^{2+} species were the active sites. Cu-SSZ-13 active sites were further investigated by Ribeiro et al.[15] who discovered that 4-fold Cu(II) and 2-fold Cu(I) species are the most stable sites contributing to SCR activity. Weng et al.[18] found that ion exchanged Cu-SAPO-34 resulted in better SCR activity than a precipitated sample; therefore they concluded that the isolated Cu ions were the active sites for NH_3−SCR. Recently, Tronconi et al.[19] developed a micro-kinetic model to predict the fast− and NO_2−SCR reaction behavior over a commercial Cu-zeolite, and they found that the reaction pathway coincided with the surface mechanism that they previously proposed for the metal-exchanged ZSM-5 catalyst.

The above-mentioned work has focused on material characterization and confirmation of the transition metal active sites in Cu-CHA catalysts. The present study is directed at understanding the SCR reaction mechanism on a Cu-SAPO-34 catalyst using in situ diffuse reflectance infrared Fourier transform spectroscopy (DRIFTS). The surface chemistry of the SCR reaction on Cu-SAPO-34 was investigated via identification and reactivity of the adsorbed surface species and surface reaction intermediates.

2. EXPERIMENTAL SECTION

2.1. Catalyst. The catalyst used in this study was a Cu-SAPO-34 catalyst supplied by Cummins Inc. The Cu-SAPO-34 catalyst sample had a Si/(Al+P) ratio of 0.2. The Cu loading was 0.95 wt %. For SCR activity tests, a monolithic-supported sample was used, and was 1.4″ long and 0.8″ in diameter. To prevent gas bypass, the sample was wrapped with insulation material (Tetraglas 3000) before being installed into a quartz tube reactor. The reactor was placed inside a Lindberg temperature-controlled furnace. Small quartz tubes were positioned upstream of the catalyst to improve gas distribution and preheating. Four thermocouples were inserted to monitor the temperatures at positions upstream, front-face center, back-face center, and back-face outer edge of the monolith. The temperature differences during all experiments were less than 4 °C. Therefore, the averages of these four temperatures were used when analyzing the data and in the figures presented. Before testing, the catalyst was degreened at 650 °C for 4 h in flowing 8% O_2, 5% H_2O, and a balance of N_2.

For the pilot-reactor experiments, all gases except N_2 were supplied by Praxair and were metered by MKS mass flow controllers. Balance N_2 was produced by a N_2 generator manufactured by On-Site. Water was injected using a Bronkhorst CEM system. All the lines were heated and maintained at 130 °C to prevent water condensation. NH_3 was introduced directly into the reactor via a three-way valve at the reactor inlet to prevent reaction along upstream tubing and to reduce the response time. The effluent gas concentration was measured using a FTIR analyzer (MultiGas 2030). The simulated exhaust gas contained 500 ppm NO, 500 ppm NH_3, 8% O_2, and 5% H_2O with a balance of N_2. The total flow rate was 5 L/min, and the corresponding gas hourly space velocity (GHSV) was 28000 h^{-1}. The NO and NH_3 conversions were calculated using the following equations:

$$X_{NO} = \frac{C_{NO_{x_{in}}} - C_{NO_{x_{out}}}}{C_{NO_{in}}} \times 100\%$$

$$X_{NH_3} = \frac{C_{NH_{3_{in}}} - C_{NH_{3_{out}}}}{C_{NH_{3_{in}}}} \times 100\%$$

In situ DRIFTS experiments were performed using a Nicolet 6700 spectrometer equipped with a MCT detector and a high temperature reaction chamber (Harrick Scientific Praying Mantis) with ZnSe windows. The powder sample was scraped from the monolith sample and was pressed into a 60 mg pellet of 6.5 mm diameter and placed in the sample cup with a porous screen at the bottom surface, allowing the gas to uniformly pass through the catalyst from top to bottom. The sample was heated by a cartridge heater underneath the support, and the temperature was adjusted using a K-type thermocouple connected to a Harrick temperature controller. The total flow rate of the stream was maintained at 50 cm^3/min (STP) with MKS mass flow controllers. At the same time, the effluent gas composition from the DRIFTS cell was measured using a mass spectrometer (Pfeiffer Vacuum OmniStar). NH_3 (m/e = 17), NO (m/e = 30), N_2 (m/e = 28), and N_2O (m/e = 44) were specifically monitored. Prior to each test, the catalyst sample was pretreated at 600 °C in a flow of 5% O_2 in He for 30 min and then cooled to the target temperature. Background spectra were recorded in flowing He and subtracted from the sample spectrum for each measurement. The DRIFTS spectra were collected in the range of 4000−650 cm^{-1} by accumulating 64 scans at a 4 cm^{-1} resolution. Nicolet OMNIC software was used to convert the absorbance data into Kubelka−Munk (KM) format. For temperature-programmed desorption (TPD) experiments, background spectra were collected in He every 50 °C from 100 to 500 °C. During the temperature ramp reaction experiments, DRIFTS spectra were recorded every 50 °C, and the corresponding backgrounds were then subtracted. It should be pointed out that all the DRIFTS experiments were performed in the absence of water, in this case because of its wide interference of the IR bands. However, it is noted that the inclusion of water may competitively adsorb on the catalyst surface and hinder NH_3 or NO_x adsorption. We assume that the surface intermediates observed and the global reaction mechanism still apply to the exhaust feed in the presence of water.

dx.doi.org/10.1021/cs300843k | ACS Catal. 2013, 3, 871−881

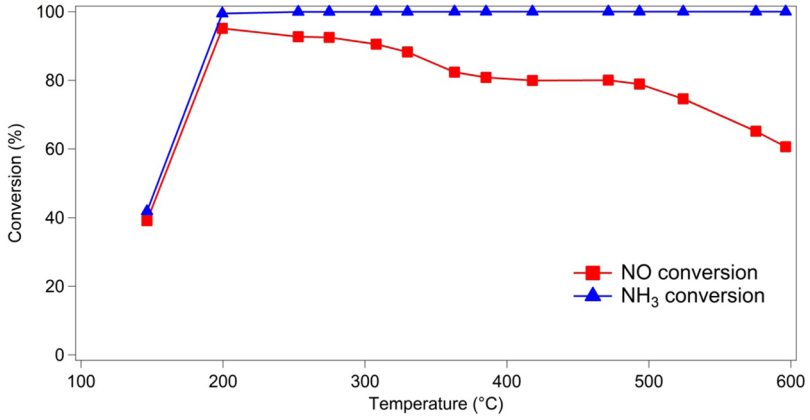

Figure 1. NO and NH_3 conversion under "standard SCR" conditions (500 ppm NO + 500 ppm NH_3 + 8% O_2 + 5% H_2O in N_2) over Cu/SAPO-34 (GHSV: 28000 h^{-1}).

3. RESULTS AND DISCUSSION

3.1. Activity Measurements. The standard SCR reaction activity was evaluated over the monolith-supported Cu-SAPO-34 catalyst from 150 to 600 °C, and the NO and NH_3 conversion results are shown in Figure 1. About 40% NO conversion was achieved at 150 °C. The maximum NO conversion (95%) occurred at 200 °C. With increasing temperature from 200 °C, the conversion decreased because of the competitive NH_3 oxidation reaction at high temperature, as evidenced by 100% NH_3 conversion at these temperatures. In addition, very little N_2O (<5 ppm) and NO_2 (<20 ppm) were detected during these tests, indicating a high selectivity of NO to N_2 was achieved. In terms of NO_2, it would be expected that any formed would participate in the fast SCR reaction and thus be consumed, leading to its absence at the outlet.

3.2. NO_x Adsorption. To investigate the interaction of NO_x with the Cu-SAPO-34 surface, the catalyst sample was exposed to NO, NO + O_2, and NO_2 in He for 30 min and then purged with pure He for 30 min at 100 °C. The DRIFTS spectra are shown in Figure 2. NO, NO + O_2, and NO_2 adsorption resulted in three common bands at ~1625, 1610, and 1602 cm^{-1}. Two additional bands at 1575 and 1530 cm^{-1} were present only when NO + O_2 or NO_2 were introduced. The bands in the range of 1650 cm^{-1}–1500 cm^{-1} are widely accepted to be the surface nitrate or nitro species adsorbed primarily on the transition metal active sites of catalyst.[20−22] However, accurate identification of these bands is not straightforward because of the similar vibrations of different nitrate structures (monodentate, bridging monodentate, chelating bidentate, and bridging bidentate species).[21,22] For example, Long and Yang observed two bands, at 1622 cm^{-1} and 1568 cm^{-1}, upon NO_2 exposure to NH_3 preadsorbed on Fe-ZSM-5, and they assigned these bands to adsorbed NO_2 and nitrate species, respectively.[5] Ruggeri et al. observed similar bands at 1620 cm^{-1} and 1574 cm^{-1} with Fe-ZSM-5 and assigned both of them to bridging or bidentate nitrate species on Fe^{3+} ions.[10] Rivallan et al. compared the adsorbed NO_2 species on H-ZSM-5, silicalite, Fe-silicalite, and Fe-ZSM-5.[23] They concluded that the band at 1658 cm^{-1} was due to NO_3^- species that formed by NO_2 attaching to the SiO*Si group, the band at 1635 cm^{-1} was due to NO_3^- species formed on FeO*Al groups, and the features between 1580 and 1620 cm^{-1} were due to nitrate-like species on FeOSi bridges, and the shift from 1620 cm^{-1} to 1610 cm^{-1} due to the formation of a $NO_3^-(N_2O_4)$ complex. Adelman et al. observed three bands in the same region when characterizing Cu-ZSM-5, and they attributed the bands at 1628, 1594, and 1572 cm^{-1} to a nitro group, a bridging monodentate nitrate, and a bidentate nitrate, respectively.[24] By analogy with the assignments of adsorbed NO_x species on other zeolites, the bands at 1625 cm^{-1}, 1610 cm^{-1} (and 1602 cm^{-1}), and 1575 cm^{-1} (and 1530 cm^{-1}) can be

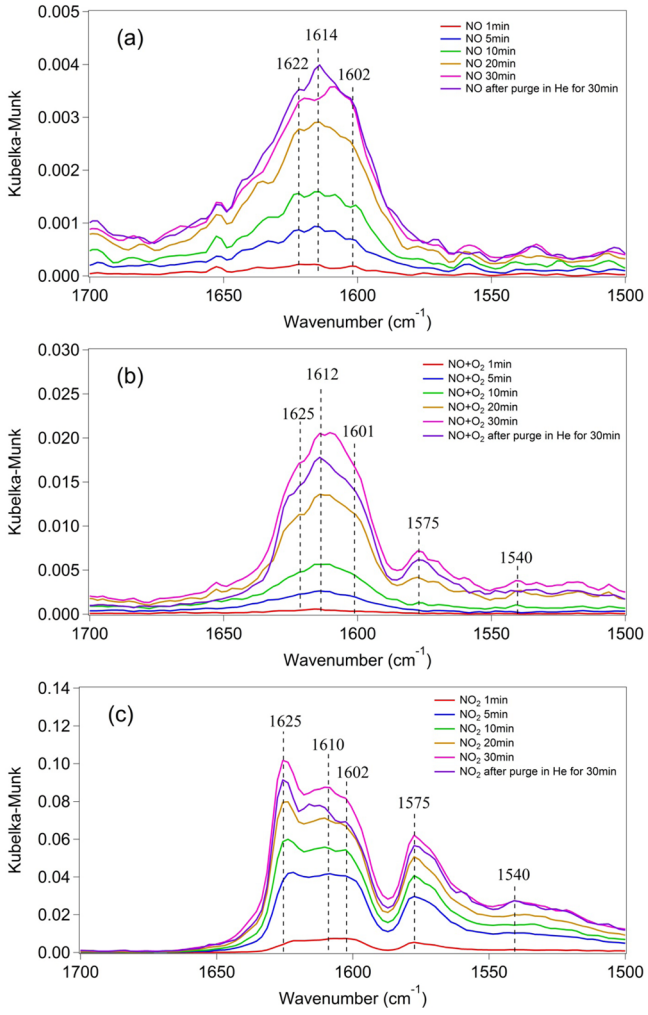

Figure 2. DRIFTS spectra obtained after exposing the Cu-SAPO-34 sample, for 30 min at 100 °C, to (a) 500 ppm NO; (b) 500 ppm NO + 5% O_2; (c) 500 ppm NO_2; followed by a 30 min exposure to He only.

dx.doi.org/10.1021/cs300843k | ACS Catal. 2013, 3, 871−881

tentatively assigned to adsorbed NO_2 species, monodentate nitrates, and bidentate nitrates, respectively. These nitrate species were relatively stable as all these bands maintained their intensities during subsequent exposure to just He. By comparing the intensities of the NO_3^- bands detected upon passing NO, NO + O_2, and NO_2 over the catalyst surface, it is obvious that the NO_3^- concentrations that formed on the surface are in the order of NO_2 > NO + O_2 > NO. This strongly indicates that NO oxidation to NO_2 would promote the formation of surface nitrates. Indeed, NO_2 was produced in the full temperature window when 500 ppm NO and 5% O_2 were introduced over the monolithic Cu-SAPO-34 catalyst (Supporting Information, Figure S1). In addition, our NO_2-TPD experiment (data not shown here) shows that Cu-SAPO-34 could adsorb a large amount of NO_2 in the form of nitrates on the surface, which were still evident above 400 °C. However, the amount of adsorbed NO was significantly lower. This is consistent with the NO_x adsorption properties reported on a Cu-ZSM-5 catalyst.[25] Many authors have agreed that NO oxidation to NO_2 is a key factor for surface nitrate formation under standard SCR conditions and therefore it is considered a crucial step for NH_3–SCR.[25−27] NO oxidation is inhibited by NO_2, which is found to be more stably adsorbed on Cu-Chabazite than on Fe-ZSM-5.[26] This appears to explain the lower NO oxidation activity on Cu-SAPO-34. It is worth pointing out that no peaks related to nitrite species were detected. This could be due to the fact that surface nitrite bands, which are usually found in the 1440 to 1100 cm^{-1} range, were obscured by the asymmetric stretching framework modes in the same region.[10,21,28] In fact, a small band at around 1350 cm^{-1} was observed during NO_x adsorption, which could be assigned to nitrite groups;[28] however, this band was too weak to be assigned with certainty. In addition to surface nitrate species, a broad band between 2100 cm^{-1} and 2200 cm^{-1} was detected. This band was reversible once the NO_x flow was turned off, and therefore was attributed to NO^+ species that weakly adsorbed on acid sites. A similar assignment has been reported by many authors.[20,22,23,28] Additionally, a weak band at 1903 cm^{-1} was detected upon exposure to NO, and this is assigned to mononitrosyl species on Cu^{2+} sites.[29] In the OH stretching region (4000 cm^{-1} to 2400 cm^{-1}), bands at 3740, 3679, 3657, and 3560 cm^{-1} were observed and attributed to perturbed Si–OH, P–OH, and OH groups associated with the extra-framework Al and Cu, respectively.[18,28,30,31] The weak negative bands at 3627 and 2599 cm^{-1} originated from the depletion of Brønsted acid sites (Si–OH–Al) by NO^+. This assignment is confirmed via evolution of a similar band at 2145 cm^{-1}, which corresponds to NO^+ on acid sites. Upon exposure to NO_2, DRIFTS spectra revealed two additional peaks at 3236 cm^{-1} and 2597 cm^{-1} (data not shown). These two peaks were assigned to the first overtone band and combination band of a NO_2 group (1625 cm^{-1}), respectively.[32,33]

3.3. NH_3 Adsorption and NH_3-TPD. The catalyst sample was exposed to 500 ppm NH_3 in He for 30 min at 100 °C and then purged in He for 30 min at the same temperature. The DRIFTS spectra collected during exposure to NH_3 are shown in Figure 3. A major band at 1460 cm^{-1} and a weak band at 1617 cm^{-1} were immediately detected after introducing NH_3 for 1 min. The former is assigned to NH_4^+ species resulting from NH_3 adsorbed on Brønsted acid sites including terminal Si–OH, P–OH groups, and bridging OH sites (Al–OH–Si) on SAPO-34.[18,34] The band at 1617 cm^{-1} is attributed to molecularly adsorbed NH_3 on Lewis acid sites.[18,34] It has been

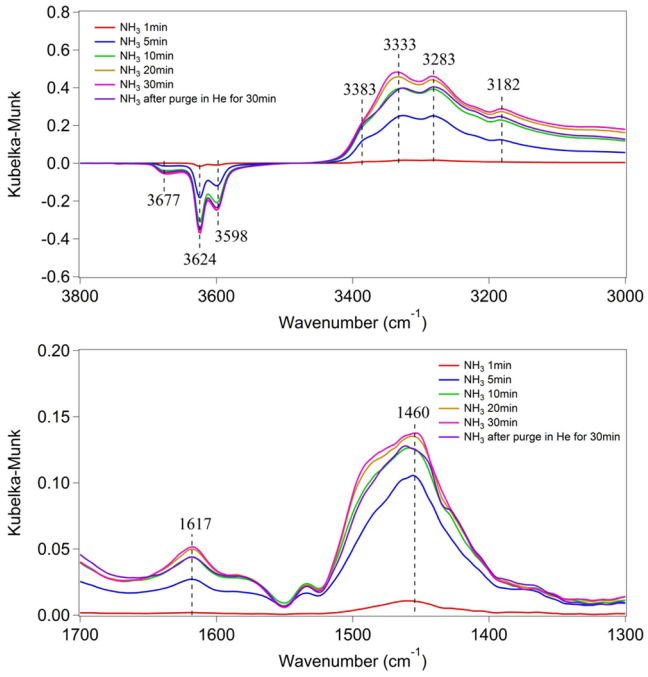

Figure 3. DRIFTS spectra obtained after exposing the Cu-SAPO-34 sample to 500 ppm NH_3 for 30 min followed by exposure to only He for 30 min, at 100 °C.

cited that Lewis acid sites are primarily composed of the transition metal ions in metal ion exchanged zeolites,[18,35,36] while some extra-framework Al, mostly located at the external surface of the zeolite, may also contribute to the number of Lewis acid sites.[37−39] After a 20 min exposure, both Brønsted acid sites and Lewis acid sites were saturated with NH_3. During the following purge with He, a small amount of NH_3 adsorbed on the weak acid sites was removed, resulting in a slight decrease in the bands 1460 cm^{-1} and 1617 cm^{-1}. In the OH stretching region, negative bands at 3677, 3624, 3598 cm^{-1} were observed. The negative band at 3677 cm^{-1} is assigned to the occupation of P–OH sites by NH_3, reducing the corresponding OH stretching vibrations, and the two other bands are attributed to the depletion of Si–OH–Al acid sites by NH_3.[18] The different IR bands corresponding to Si–OH–Al sites were due to the OH groups with equal acidity strengths that are located in various oxygen environments in the chabazite framework.[40] A band at 3740 cm^{-1} was also detected upon exposure to NH_3 at room temperature, and can be assigned to NH_3 adsorbed onto Si–OH groups.[18] This, however, was not observed in the NH_3 adsorption spectra taken at temperatures higher than 100 °C because of the weak adsorption strength of NH_3 on this site. In addition, positive bands at 3333, 3383, 3283, and 3182 cm^{-1} were detected. The bands in the 3400 to 3000 cm^{-1} range are often assigned to N–H stretching vibrations.[22,41] Specifically, bands at 3333 cm^{-1} and 3283 cm^{-1} have been assigned to NH_4^+ groups.[11] The band at 3383 cm^{-1} has been attributed to NH_3 molecules and the band at 3182 cm^{-1} due to NH_3 adsorbed on Cu^+ sites on SAPO-34.[18,22,34,42] It is worth noting that all of these NH_3 adsorption species were relatively stable at 100 °C after turning off NH_3 and purging in He.

The NH_3 adsorption process was followed by a temperature-programmed desorption (TPD) experiment to study the NH_3 adsorption strength and acid properties of the Cu-SAPO-34

dx.doi.org/10.1021/cs300843k | ACS Catal. 2013, 3, 871−881

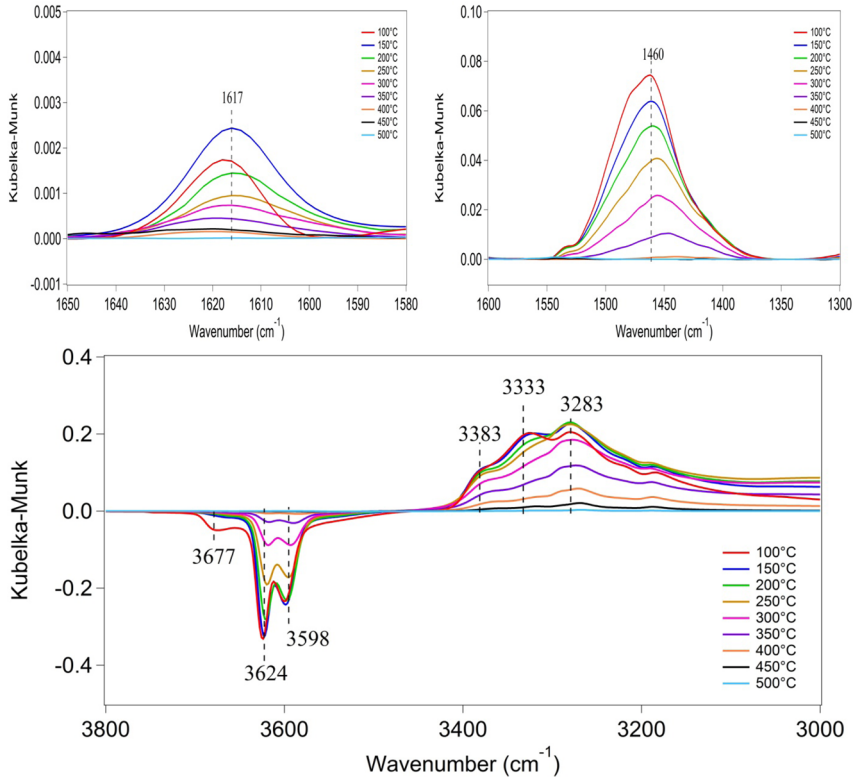

Figure 4. DRIFTS spectra obtained during a TPD (10 °C/min) after the sample had been exposed to 500 ppm NH_3/He, followed by a He-only exposure for 30 min.

sample. Representative DRIFTS spectra collected at different temperatures, with a 10 °C/min ramp from 100 to 500 °C, are shown in Figure 4. At the beginning of the temperature ramp, the intensity of the 1460 cm^{-1} feature decreased because of NH_3 desorption from weak Brønsted acid sites. Interestingly, the intensity of the band at 1617 cm^{-1} increased between 100 and 150 °C, and then decreased with increasing temperature. This indicates that some of the NH_3 that desorbed from weak Brønsted acid sites or from P−OH like species might have readsorbed onto the Lewis acid sites in this low temperature region. Indeed, a significant reduction of the 3677 cm^{-1} band, which was assigned to the weak Brønsted acid P−OH group, was observed in the corresponding DRIFTS spectra. To more clearly evaluate the evolution of NH_3, the normalized peak areas of each key band were calculated and are shown in Figure 5. As shown in Figure 5, NH_4^+ and Al-OH-Si feature intensities followed a monotonic decreasing trend with increasing temperature. This demonstrates that the OH bridging band is the major source of Brønsted acid sites on Cu-SAPO-34. Furthermore, both 3598 and 3624 cm^{-1} bands, corresponding to Brønsted acid sites, decreased in unison (Figure 4) indicating these two acid sites are energetically similar. Figure 5 clearly shows the significant increase in the size of the feature associated with the increase in the NH_3 concentration on Lewis acid sites at 150 °C because of readsorption of NH_3 released from other acid sites as suggested above. At temperatures above 200 °C, NH_3 desorbing from Brønsted acid sites and Lewis acid sites showed analogous profiles, indicating that both types of sites have similar acid strengths on Cu-SAPO-34. This is inconsistent with the findings from studies of other metal exchanged zeolites which showed distinctly different Lewis and Brønsted acid site strengths.[35,36,38,43] This unique acidity might be a crucial feature contributing to the SCR activity of Cu-

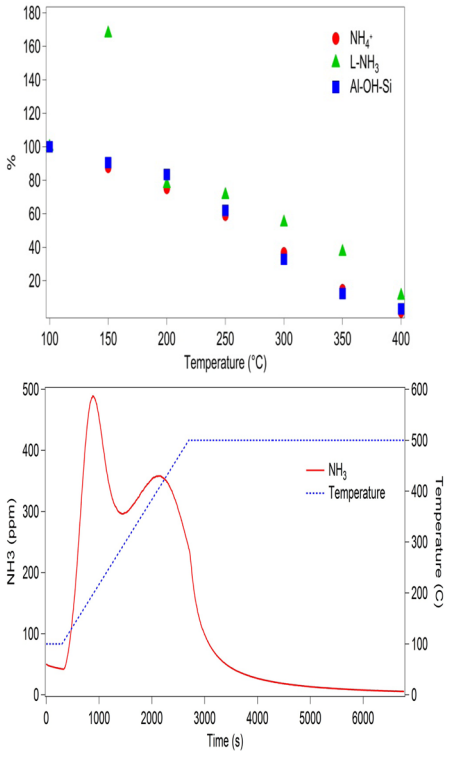

Figure 5. Normalized DRIFTS peak intensities during the TPD (Figure 4), and NH_3 evolved.

SAPO-34, as it facilitates NH_3 migration between the two acid site types, potentially enabling more NH_3 to be transferred to the transition metal NO_x reduction reaction site. The outlet

dx.doi.org/10.1021/cs300843k | ACS Catal. 2013, 3, 871−881

NH_3 concentrations as a function of temperature are also shown in Figure 5. The NH_3 desorption profile has two main desorption features, a narrow low temperature peak at about 200 °C and a broad high temperature peak at 400 °C. Via comparison with the DRIFTS spectra during the NH_3 desorption process, the low temperature peak is attributed to the weak acid sites (P−OH and extra-framework Al) and physisorbed NH_3. The broader peak at high temperature is attributed to NH_3 desorbed from Cu^{2+} Lewis acid sites and OH bridging Brønsted acid sites. No distinct features in the NH_3 desorption profile above 200 °C further supports the energetically indistinguishable two acid site types on Cu-SAPO-34 as evident from DRIFTS spectra.

3.4. Reactivity of NH_3 on Cu-SAPO-34. As shown in Figure 1, the best NO reduction performance was measured at 200 °C; therefore NH_3 reactivity DRIFTS studies were also carried out at 200 °C. DRIFTS spectra obtained during the reaction between NO and preadsorbed NH_3 at 200 °C are shown in Figure 6. Upon exposure to 500 ppm NO, slight

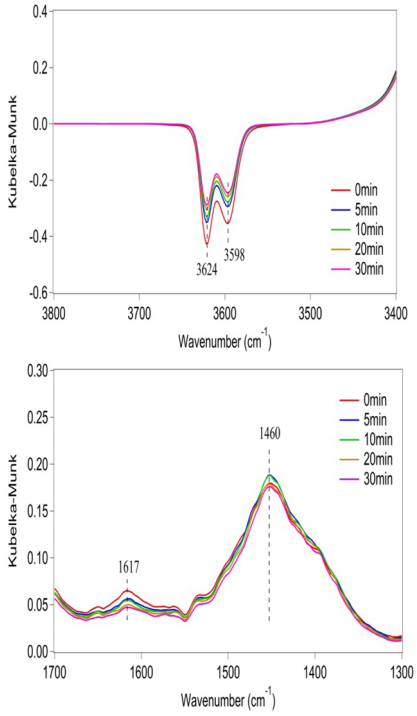

Figure 6. DRIFTS spectra obtained at 200 °C while exposing the Cu-SAPO-34 sample to 500 ppm NO/He after being saturated with NH_3.

decreases in the OH bridging band (3624 cm^{-1} and 3598 cm^{-1}) and the band (1617 cm^{-1}) assigned to NH_3 on Lewis acid sites were detected. Simultaneously, only a small amount of N_2 was detected in the outlet, indicating that NO itself was not active in reacting with surface NH_3. In comparison, when 500 ppm NO and 5% O_2 were passed over the NH_3 preadsorbed catalyst sample at 200 °C, the surface NH_3 was consumed at a significantly increased rate, as shown in Figure 7. After 30 min, all bands related to NH_3 were greatly reduced, which was also accompanied by a significantly larger amount of N_2 in the outlet gas, observed over the entire 30 min exposure to NO + O_2. Obviously, the SCR reaction activity was enhanced by the addition of O_2 in the feed, that is, the reaction between NH_3 and NO is promoted by NO oxidation, enhancing the storage of surface nitrates and nitrites on the

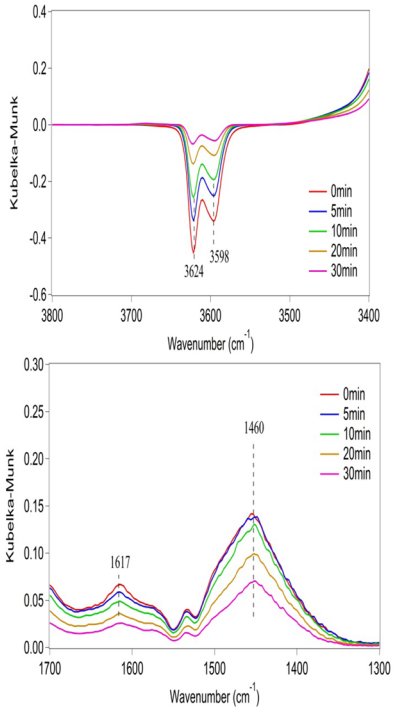

Figure 7. Evolution of (a) -OH bridging bond peaks; and (b) peaks of NH_3 on Lewis acid sites and Brønsted acid sites; upon exposure to 500 ppm NO + 5% O_2 at 200 °C.

catalyst surface. Indeed, similar results have been obtained on other SCR catalysts, and it is widely accepted that NO has to be first oxidized to NO_2 (gas-phase or some oxidized surface species) for the standard SCR reaction over zeolite catalysts.[1,5,11,44] Normalized peak areas were used to evaluate the reactivity of NO + O_2 with NH_3 adsorbed on different sites. As shown in Figure 8, both NH_3 adsorbed on Lewis acid sites and OH bridging bond sites show a relatively linearly decreasing trend. However, the IR band intensity corresponding to NH_4^+ did not change in step with Brønsted acid sites. This additional NH_4^+ must originate from another source of NH_3 on the catalyst surface. Since NH_3 exists as NH_4^+ or molecular NH_3 on the surface, as demonstrated in the NH_3 adsorption study, the only possibility is that some NH_3 bound to the Lewis acid sites is protonated and transformed into NH_4^+ species during the interaction with NO + O_2. Interestingly, no such NH_4^+ evolution was observed during exposure to NO.

To clarify the origin of this evolution, 500 ppm NO_2 was passed over the NH_3 preadsorbed catalyst sample at 100 °C. Using a lower temperature potentially allows the capture of the reaction intermediate on the surface that was produced during the reaction. As shown in Figure 9, the NH_3 adsorbed on P−OH (3677 cm^{-1}) and OH bridging sites (3624 and 3598 cm^{-1}) were gradually consumed during exposure to NO_2 for 30 min. On the other hand, the intensity of band at 1617 cm^{-1}, associated with the NH_3 adsorbed on Lewis acid sites, rapidly decreased and completely disappeared after 5 min. However, the NH_4^+ vibration mode significantly increased for the first 10 min and slightly decreased subsequently. Surface nitrates, with a band at 1575 cm^{-1}, appeared after 10 min, and the intensity of the DRIFTS feature increased over the remaining 20 min exposure. In addition to the surface NH_3 and nitrates species (bands at 1617, 1575, and 1460 cm^{-1}), a new band at 1596 cm^{-1} was detected after 10 min. The initial increase of NH_4^+

dx.doi.org/10.1021/cs300843k | ACS Catal. 2013, 3, 871−881

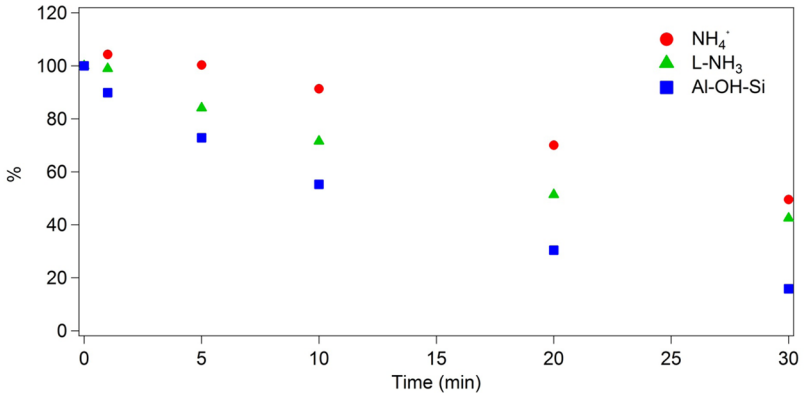

Figure 8. Normalized peak intensities associated with the DRIFTS results shown in Figure 7.

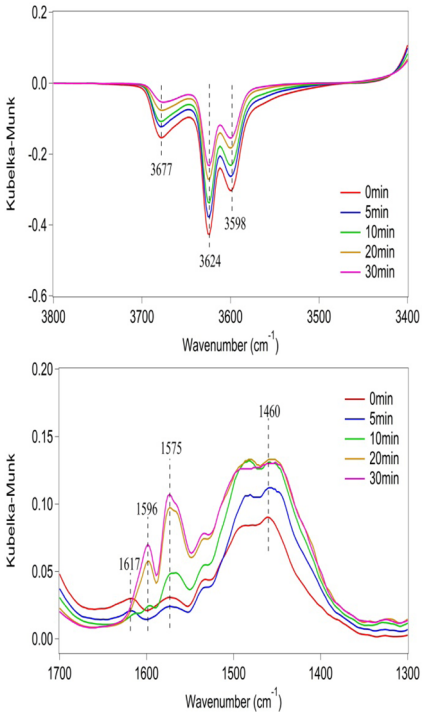

Figure 9. DRIFTS spectra obtained at 100 °C during exposure to 500 ppm NO_2/He after presaturating with NH_3.

band was very likely due to the formation of NH_4NO_2 which caused the elevation of NH_4^+ during the first 10 min. However, with further exposure to NO_2, NH_4NO_2 surface species could be oxidized to NH_4NO_3, which is explained by the appearance of bands at 1575 cm^{-1} and 1596 cm^{-1} after 10 min in the DRIFTS spectra. As indicated by the normalized peak areas (Figure 10), the bands at 1596 cm^{-1} and 1575 cm^{-1} showed a very similar trend, suggesting that they might originate from the same surface intermediate, likely NH_4^+-NO_3^- species. Indeed, similar surface species have been found on many other SCR catalysts upon exposure to NH_3 and NO_2. For example, Long and Yang detected a reaction intermediate with a band of 1602 cm^{-1} when NO_2 was introduced onto an NH_3-adsorbed Fe-ZSM-5 sample, and they predicted this band to be an $NO_2(NH_4^+)_2$ like species.[5] Nova et al. found an intense band at 1380 cm^{-1} upon passing NH_3 and NO_2 over a V_2O_5–WO_3/TiO_2 catalyst at 140 °C. They assigned this peak to an NH_4NO_3 deposit since the IR spectrum of pure NH_4NO_3 contains the same peak.[45] Malpartida et al.[46] reported that the activity of a commercial zeolite-based catalyst was decreased by the formation of NH_4NO_3 deposits when passing NO_2 over an NH_3 preadsorbed sample, which was evidenced by comparing the operando IR spectra of a NH_4NO_3 mixed sample with the spectra taken during a test with NO_2 at 165 °C. On the other hand, it is obvious that the increase in NH_4^+ was more distinct compared with that during exposure to NO + O_2. This further suggests that the higher level of nitrate and nitrite species formed upon NO_2 adsorption facilitates the transformation of molecular NH_3 adsorbed on Lewis acid sites to the NH_4^+-NO_x species that enhances the NH_4^+ signal. Since molecular NH_3 only exists on the Lewis acid sites, it is reasonable to believe that the formation of this intermediate occurred on Lewis acid

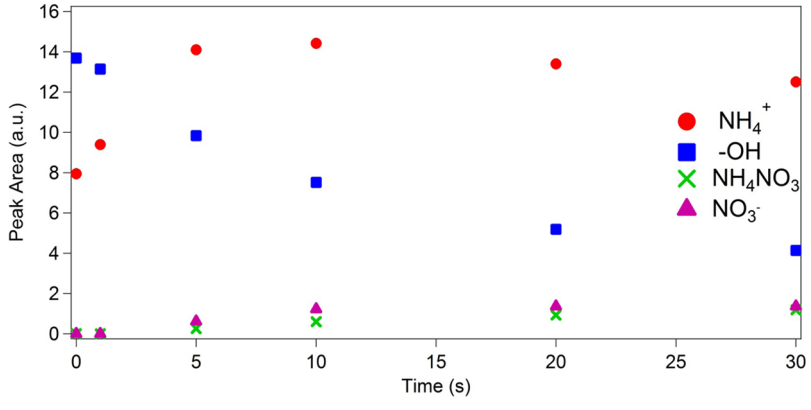

Figure 10. Normalized peak areas, associated with the DRIFTS results shown in Figure 9.

dx.doi.org/10.1021/cs300843k | ACS Catal. 2013, 3, 871–881

sites. Meanwhile, the NH_3 on Brønsted acid sites might migrate to Cu sites and supply NH_3 for reaction, which coincides with the hydroxyl IR bands approaching the baseline. Indeed, the change in the band corresponding to NH_4^+ was in fact not in step with OH group changes, further indicating that NH_4NO_3 was perhaps not interacting with Brønsted acid sites, at least not very strongly. It seems reasonable that this kind of migration could be facilitated by the small pores of the SAPO-34 material in which the distance between the Brønsted acid sites and Lewis acid sites is small. Interestingly, the band at 1596 cm^{-1} was not observed upon exposure to NO + O_2 on the sample with preadsorbed NH_3. This could be explained by the following: first, as shown in Figure 2, a significantly larger amount of surface nitrates was formed by NO_2 compared to NO + O_2. In other words, this intermediate was promoted by the presence of surface NO_3^-. Second, this intermediate and surface nitrate could be quickly reduced by NO and therefore were not observed on the surface. Indeed, when we exposed the NH_3 preadsorbed samples to 500 ppm NO + 50 ppm NO_2 at the same temperature (50 ppm NO_2 could be generated at 200 °C via NO oxidation as shown in Supporting Information, Figure S1), no band at 1596 cm^{-1} was detected in the DRIFTS spectra (Supporting Information, Figure S2). This provides strong evidence that NO_2 was either first formed and stored on the surface followed by formation of NH_4^+-NO_x (x = 2 or 3) or nitrates were formed via oxidation of surface NO_x species and then NH_4^+-NO_x formed, which could be easily reduced by NO under standard SCR inlet conditions.

3.5. Confirmation of the NH_4NO_3 Intermediate. To identify the intermediate, a TPD experiment was conducted after it was formed. The DRIFTS spectra and outlet concentrations of different species are shown in Figure 11. During the temperature ramp, the band at 1596 cm^{-1}, which corresponded to the deposit formed by surface NH_3 and NO_3^-, decreased in intensity starting from 200 °C and was completely removed from the surface by 500 °C. Concurrently, a significant amount of N_2O was observed in the outlet gas starting at about 200 °C. According to literature,[1,44,47] N_2O originates from NH_4NO_3 at low temperature and NH_3 oxidation at higher temperature, and since 200 °C is the onset temperature of the NH_4NO_3 decomposition reaction these results suggest it is a major reaction intermediate present on the catalyst.

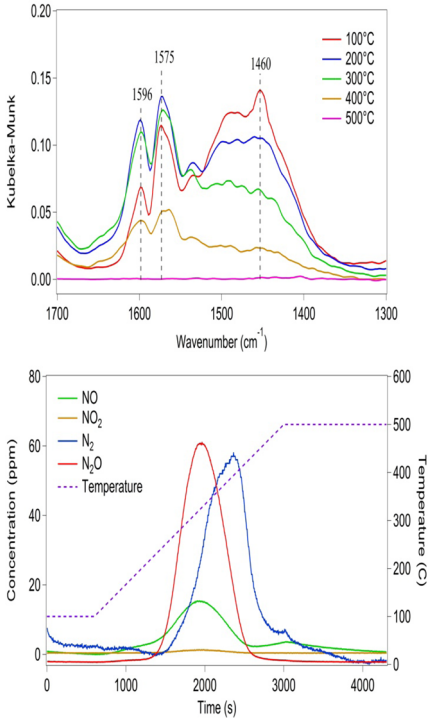

Figure 11. DRIFTS spectra obtained during a TPD (in He, 10 °C/min) after exposing the NH_3-presaturated sample to 500 ppm NO_2/He.

During the temperature ramp, no NH_3 evolution was detected in the outlet gas, meaning that all the NH_3 was involved in combining with nitrates that stored on the surface and formed NH_4NO_3. This result is consistent with a similar study conducted on Fe-ZSM-5 which concluded that the NH_3 spills over to the nitrates that formed during NO_2 adsorption and only NH_4NO_3 species were present on the catalyst.[47] Interestingly, the band at 1596 cm^{-1} initially increased with increasing temperature, from 100 to 200 °C. This might be attributed to enhanced mobility of NH_3 at higher temperature that enables more NH_3 to reach Lewis acid sites to form the NH_4NO_3 intermediate. To further confirm the formation of NH_4NO_3 on the surface, a DRIFTS single beam spectrum was taken on a fresh Cu-SAPO-34 sample that was mechanically mixed with NH_4NO_3 powder (Sigma Aldrich) to attain a 3 wt % NH_4NO_3 mixture. By subtracting this spectrum of a pure Cu-SAPO-34 sample at the same temperature, the NH_4NO_3 species that stored on the surface of the catalyst might be distinguished. Figure 12 compares the spectrum of the

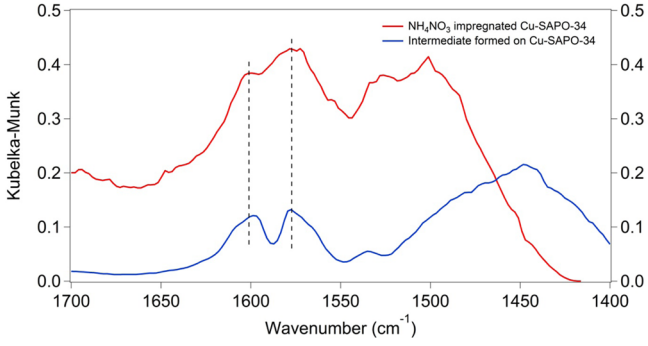

Figure 12. Comparison of DRIFTS spectra of a fresh Cu-SAPO-34 catalyst sample impregnated with NH_4NO_3 and the sample after exposure to NH_3 and NO_2 at 100 °C.

impregnated sample with the one taken at 100 °C after exposing the Cu-SAPO-34, with preadsorbed NH_3, to NO_2 for 30 min. It is evident that the bands at 1596 and 1575 cm^{-1} appeared in both spectra and their positions closely match, providing further evidence for the assignments of these bands to NH_4NO_3. To investigate the role of NO in the SCR reaction, 500 ppm NO was passed over the sample containing NH_4NO_3 at 100 °C. As shown in Figure 13, the bands at 1596, 1575, and 1460 cm^{-1}, being indicative of NH_4NO_3 and NH_4^+, were significantly decreased after 30 min. N_2 was detected in the outlet over the entire 30 min period. This further proves that this surface intermediate is very active in reacting with gaseous NO, reacting to N_2 at as low a temperature as 100 °C.

3.6. Reaction Pathway. As discussed above, the SCR reaction starts with NO oxidation, to produce gas-phase NO_2, which could easily adsorb and store on the Cu-SAPO-34 catalyst in the form of surface nitrates and nitrites. These

dx.doi.org/10.1021/cs300843k | ACS Catal. 2013, 3, 871−881

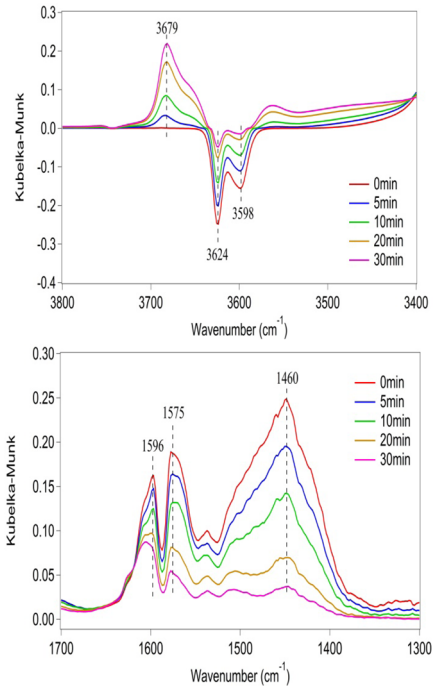

Figure 13. DRIFTS spectra obtained at 100 °C during exposure to 500 ppm NO, after the NH_3 saturated sample had been exposed to 500 ppm NO_2/He.

surface nitrate and nitrite species were produced through NO_2 dimerization and disproportionation:

$$2NO + O_2 \leftrightarrow 2NO_2 \quad (1)$$

$$2NO_2 \leftrightarrow N_2O_4 \quad (2)$$

$$N_2O_4 \leftrightarrow NO_3^- + NO^+ \quad (3)$$

Reactions 2 and 3 have been extensively reported for the formation of surface NO_3^- and NO_2^- species on other zeolite catalyst systems.[31,48,49] The observation of a broad peak at around 2144 cm^{-1} in our spectra confirmed the existence of NO^+ ions on Cu-SAPO-34. It has also been proposed by many authors[23,50,51] that NO^+ may incorporate with surface oxygen or coordinated oxygen to form NO_2^- species according to reaction 4. The existence of coordinated oxygen (lattice O^{2-} or OH^-) has been confirmed using density functional theory (DFT), electron paramagnetic resonance (EPR), and synchrotron-based techniques, and research has shown that isolated Cu^{2+} could associate with at most four oxygen atoms under SCR conditions.[15,52,53] However, surface NO_2^- or nitrite related species are difficult to detect in our spectra due to either its overlapping regions with zeolite asymmetric vibrations or their rapid reactivity with NH_3 on the surface.

$$NO^+ + O^{2-} \leftrightarrow NO_2^- \quad (4)$$

$$NO_3^- + NO^+ + Zeo{-}O{-}H \leftrightarrow Zeo{-}O{-}NO^+ + HNO_3 \quad (5)$$

NO^+ produced from NO_2 dimerization and disproportionation was found to replace the proton on Brønsted acid sites and forms HNO_3 species according to reaction 5.[23] This replacement is evidenced by the evolution of negative bands associated with OH bridging bonds when NO, NO + O_2, or NO_2 was passed over the catalyst, as shown in Figure 2. The existence of HNO_3 has been reported by Rivallan et al., who observed a broad NO_2 adsorption band that covers the whole 1650−1450 cm^{-1} region on H-ZSM-5 and attributed this band to be neutral weakly adsorbed HNO_3 species.[23] Indeed, a similar broad band that spans the whole nitrate adsorption region was also detected in our DRIFTS spectra upon NO_2 exposure and adsorption (Figure 2). Therefore, HNO_3 is apparently present on Cu-SAPO-34 as well. Ahrens et al. have concluded HNO_3 is the main NO_2 adsorption species on Fe-ZSM-5 and Fe-BEA catalysts.[54] It is also worth pointing out that the HNO_3 may be formed via a H_2O-involved reaction as reported elsewhere.[27,54]

$$2NO_2 + H_2O \leftrightarrow HNO_3 + HNO_2 \quad (6)$$

However, as the DRIFTS experiment operating conditions used here do not include water, this reaction may not be relevant in our study. Moreover, in a separate experiment, significant gas-phase NO evolution was immediately observed when exposing Cu-SAPO-34 to NO_2 (monolith-supported sample, data shown in Supporting Information, Figure S3). This could be explained by reaction 7 or 8, in which the surface NO_2^- and HNO_2 species were further oxidized to NO_3^- (or HNO_3) by NO_2.[27,28,55] Conversely, NO_2 could be observed as well when NO was passed over NO_3^- (or HNO_3) preadsorbed Cu-SAPO-34, via the reversibility of reactions 7 and 8. Thus, both nitrate and nitrite species might exist on the catalyst surface and their proportions are primarily determined by the NO_2/NO_x ratio in the feed.

$$NO_2 + NO_2^- \leftrightarrow NO + NO_3^- \quad (7)$$

$$NO_2 + HNO_2 \leftrightarrow NO + HNO_3 \quad (8)$$

The reduction of these surface nitrate species by NO has been considered the key step for SCR activity on other catalysts, since it transforms surface NO_3^- to NO_2^- (or HNO_2), which can readily react with NH_3 to form NH_4NO_2.[8,10,45,56,57]

$$NH_4^+ + NO_2^- \leftrightarrow NH_4NO_2 \quad (9)$$

$$NH_3 + HNO_2 \leftrightarrow NH_4NO_2 \quad (10)$$

The NH_4NO_2 is unstable and easily decomposes to N_2 and H_2O at temperatures above 80 °C (eq 11).[55,58]

$$NH_4NO_2 \leftrightarrow N_2 + 2H_2O \quad (11)$$

In the presence of NO_2 in the feed, surface NH_4NO_2 could be further oxidized to NH_4NO_3 according to the reaction

$$NH_4NO_2 + NO_2 \leftrightarrow NH_4NO_3 + NO \quad (12)$$

When surface nitrates were formed on the catalyst, they readily react with NH_3 preadsorbed on Cu Lewis acid sites to form NH_4NO_3 as well.

$$NH_3 + HNO_3 \leftrightarrow NH_4NO_3 \quad (13)$$

NH_4NO_3 formation has been observed on many other SCR catalyst systems (ZSM-5, V-based catalysts, and BaNa-Y catalysts) under NO_2-rich conditions[7,59,60] and is reportedly relatively stable at low temperature. It could therefore block the active sites of the SCR reaction.[7,46] At temperatures higher than 200 °C, NH_4NO_3 decomposes to N_2O and H_2O according to reaction 14.[1,44,47]

$$NH_4NO_3 \leftrightarrow N_2O + H_2O \quad (14)$$

dx.doi.org/10.1021/cs300843k | ACS Catal. 2013, 3, 871−881

N_2O is regarded as a potential greenhouse gas, and ideally none would form during the SCR reaction. N_2O was not observed in our experiments under standard SCR reaction conditions (data not shown) over all temperature ranges, providing strong evidence that NH_4NO_3 readily reacts with NO on Cu-SAPO-34 via the following reaction

$$NO + NH_4NO_3 \leftrightarrow N_2 + 2H_2O + NO_2 \quad (15)$$

Again, reaction 15 is believed to be crucial in SCR reaction chemistry since it removes surface NH_4NO_3 and continuously converts NO into N_2. The NO_2 that concurrently formed could again adsorb and react with NH_3. It has been reported that the reaction between NH_4NO_3 and NO is the rate determining step for the fast SCR reaction on Fe-ZSM-5[8] and the onset temperature is 170−190 °C.[7,55,61] However, on Cu-SAPO-34, this reaction proceeded at even lower temperature, that is, at 100 °C. The enhanced reactivity of NH_4NO_3 with NO also leads to selectivity improvement, since N_2O originates from NH_4NO_3 decomposition, but the NH_4NO_3 is consumed at low temperatures. This could also be the key factor that explains the excellent low temperature SCR reaction activity of Cu-SAPO-34. Indeed, Tronconi et al. discovered that the injection of NH_4NO_3 into the feed could significantly enhance NO_x reduction efficiency over both Fe-ZSM-5 and V_2O_5−WO_3/TiO_2 catalysts.[62,63] The NH_4NO_3 intermediate was detected on the Cu-SAPO-34 catalyst only under fast SCR reaction conditions, not under standard SCR reaction conditions. Besides, only a negligible amount of N_2O was detected under standard SCR reaction conditions, indicating that the NH_4NO_3 decomposition reaction was not significant. In other words, any NH_4NO_3 formed was quickly reduced by the larger concentration of NO under standard SCR conditions and therefore was not observed via DRIFTS on the surface. Grossale et al. proposed that NH_4NO_3 formation on the Fe-ZSM-5 was not influenced by the order of NH_3 and NO_2 adsorption.[47] Interestingly, for Cu-SAPO-34, the DRIFTS bands associated with the NH_4NO_3 intermediate were not detected when the sample was exposed to NH_3 after preadsorbing NO_2 at 100 °C (results shown in Supporting Information, Figure S4). Concurrently, some N_2 was detected in the outlet immediately after NH_3 was introduced. To explain this, NH_4NO_3 might be generated first and quickly reduced by gaseous NH_3 according to reaction 16

$$2NH_3 + 3NH_4NO_3 \leftrightarrow 4N_2 + 9H_2O \quad (16)$$

The possibility of this reaction occurring on Cu-SAPO-34 was confirmed by exposing the sample to NH_3, after NH_4NO_3 had been formed at 200 °C and all the peaks corresponding to NH_4NO_3 were reduced and completely disappeared after 20 min, as shown in Supporting Information, Figure S5. The other possibility is that gaseous NH_3 directly reacts with surface nitrates to form N_2 according to reaction 17

$$5NH_3 + 3HNO_3 \leftrightarrow 4N_2 + 9H_2O \quad (17)$$

Both reactions 16 and 17 are regarded as NO_2 SCR reactions and reportedly start between 220 to 230 °C on Fe-ZSM-5.[64] However, on Cu-SAPO-34, it again seems that the reactivity of adsorbed nitrates with NH_3 is significantly enhanced.

To summarize, the reaction mechanism of SCR on Cu-SAPO-34 can be described by Figure 14. The reaction pathway involves NH_4NO_3 intermediate formation on Lewis acid sites followed by reaction with NO to produce N_2. This reaction on Cu sites matches the SCR reaction pathway that has been previously proposed over other zeolite-based SCR catalysts. The NH_3 on Brønsted acid sites might migrate to Lewis acid sites to provide more NH_3 for reaction instead of being directly involved in the SCR reaction. NH_3 migration on Cu-SAPO-34 at low temperature is attributed to its unique acid properties and has not been observed on other zeolite-based SCR catalysts. On the other hand, the participation of nitrite species in the SCR reaction pathway is still likely to occur, even if NH_4NO_2 species were not observed in our DRIFTS spectra. This is explained by its high reactivity, which is likely also the key in the low-temperature activity of SAPO-34 SCR catalysts.

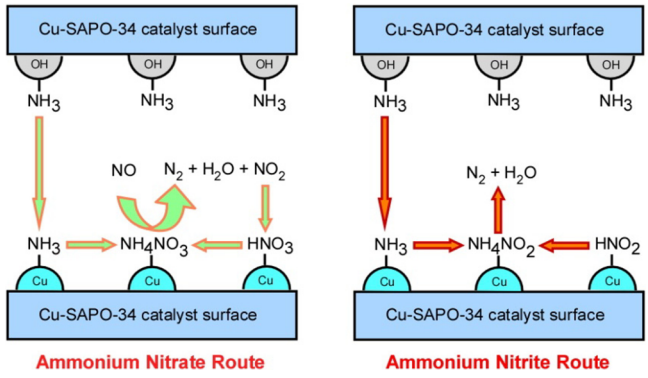

Figure 14. Proposed SCR reaction pathway on Cu-SAPO-34.

4. CONCLUSIONS

In-situ DRIFTS results show that formation of surface nitrates and nitrites is a key step in NH_3−SCR over Cu-SAPO-34. The surface nitrate and nitrite species form on the catalyst surface by dimerization and disproportionation reactions. These surface complexes readily react with surface NH_3 to form NH_4NO_2 and NH_4NO_3 on the Lewis acid sites. When NO_2 was present in the feed, NH_4NO_2 could be further oxidized to NH_4NO_3. NH_4NO_3 was reduced to N_2 in the presence of NO at temperatures as low as 100 °C, which accounts for the superior low temperature SCR reaction activity of this catalyst. The Brønsted acid sites act as an NH_3 reservoir instead of being directly involved in the SCR reaction. Actually the similar acidity strength of different acid sites on the SAPO-34 material, observed via ammonia release profiles and from IR band intensity changes during NH_3-TPD, may enable this migration. However, the possibility of NH_4NO_2 formation on Brønsted acid sites does exist as evidenced by the fast consumption of NH_4^+ species upon interaction with NO_2. Therefore, the participation of nitrite species in the SCR reaction pathway is still likely to occur, even if NH_4NO_2 species were not observed in the DRIFTS spectra, and is explained by its high reactivity.

■ ASSOCIATED CONTENT

Supporting Information

Further details are given in Figures S1−S5. This material is available free of charge via the Internet at http://pubs.acs.org.

■ AUTHOR INFORMATION

Corresponding Author

*E-mail: wsepling@uh.edu.

Notes

The authors declare no competing financial interest.

■ ACKNOWLEDGMENTS

We would like to thank Cummins Inc. for the financial support to this work.

■ REFERENCES

(1) Brandenberger, S.; Kroecher, O.; Tissler, A.; Althoff, R. *Catal. Rev.-Sci. Eng.* **2008**, *50*, 492.
(2) Long, R. Q.; Yang, R. T. *J. Catal.* **1999**, *188*, 332.
(3) Iwamoto, M.; Furukawa, H.; Mine, Y.; Uemura, F.; Mikuriya, S. I.; Kagawa, S. *J. Chem. Soc., Chem. Commun.* **1986**, *16*, 1272.
(4) Schwidder, M.; Heikens, S.; De Toni, A.; Geisler, S.; Berndt, M.; Brueckner, A.; Gruenert, W. *J. Catal.* **2008**, *259*, 96.
(5) Long, R. Q.; Yang, R. T. *J. Catal.* **2002**, *207*, 224.
(6) Metkar, P. S.; Salazar, N.; Muncrief, R.; Balakotaiah, V.; Harold, M. P. *Appl. Catal., B* **2011**, *104*, 110.
(7) Grossale, A.; Nova, I.; Tronconi, E.; Chatterjee, D.; Weibel, M. *J. Catal.* **2008**, *256*, 312.
(8) Iwasaki, M.; Shinjoh, H. *Appl. Catal., A* **2010**, *390*, 71.
(9) Grossale, A.; Nova, I.; Tronconi, E. *Catal. Today* **2008**, *136*, 18.
(10) Ruggeri, M. P.; Grossale, A.; Nova, I.; Tronconi, E.; Jirglova, H.; Sobalik, Z. *Catal. Today* **2012**, *184*, 107.
(11) Devadas, M.; Krocher, O.; Elsener, M.; Wokaun, A.; Soger, N.; Pfeifer, M.; Demel, Y.; Mussmann, L. *Appl. Catal., B* **2006**, *67*, 187.
(12) Eng, J.; Bartholomew, C. H. *J. Catal.* **1997**, *171*, 27.
(13) Fickel, D. W.; Lobo, R. F. *J. Phys. Chem. C* **2010**, *114*, 1633.
(14) Schmieg, S. J.; Oh, S. H.; Kim, C. H.; Brown, D. B.; Lee, J. H.; Peden, C. H. F.; Kim, D. H. *Catal. Today* **2012**, *184*, 252.
(15) McEwen, J. S.; Anggara, T.; Schneider, W. F.; Kispersky, V. F.; Miller, J. T.; Delgass, W. N.; Ribeiro, F. H. *Catal. Today* **2012**, *184*, 129.
(16) Kwak, J. H.; Tonkyn, R. G.; Kim, D. H.; Szanyi, J.; Peden, C. H. F. *J. Catal.* **2010**, *275*, 187.
(17) Deka, U.; Juhin, A.; Eilertsen, E. A.; Emerich, H.; Green, M. A.; Korhonen, S. T.; Weckhuysen, B. M.; Beale, A. M. *J. Phys. Chem. C* **2012**, *116*, 4809.
(18) Wang, L.; Li, W.; Qi, G. S.; Weng, D. *J. Catal.* **2012**, *289*, 21.
(19) Colombo, M.; Nova, I.; Tronconi, E. *Catal. Today* **2012**, *197*, 243.
(20) Hadjiivanov, K.; Saussey, J.; Freysz, J. L.; Lavalley, J. C. *Catal. Lett.* **1998**, *52*, 103.
(21) Hadjiivanov, K. I. *Catal. Rev.-Sci. Eng.* **2000**, *42*, 71.
(22) Sjovall, H.; Fridell, E.; Blint, R. J.; Olsson, L. *Top. Catal.* **2007**, *42−43*, 113.
(23) Rivallan, M.; Ricchiardi, G.; Bordiga, S.; Zecchina, A. *J. Catal.* **2009**, *264*, 104.
(24) Adelman, B. J.; Beutel, T.; Lei, G. D.; Sachtler, W. M. H. *J. Catal.* **1996**, *158*, 327.
(25) Olsson, L.; Sjovall, H.; Blint, R. J. *Appl. Catal., B* **2009**, *87*, 200.
(26) Metkar, P. S.; Balakotaiah, V.; Harold, M. P. *Catal. Today* **2012**, *184*, 115.
(27) Colombo, M.; Nova, I.; Tronconi, E. *App. Catal., B* **2012**, *111*, 433.
(28) Iwasaki, M.; Shinjoh, H. *J. Catal.* **2010**, *273*, 29.
(29) Szanyi, J.; Paffett, M. T. *J. Catal.* **1996**, *164*, 232.
(30) Li, G. H.; Larsen, S. C.; Grassian, V. H. *J. Mol. Catal A: Chem.* **2005**, *227*, 25.
(31) Sedlmair, C.; Gil, B.; Seshan, K.; Jentys, A.; Lercher, J. A. *Phys. Chem. Chem. Phys.* **2003**, *5*, 1897.
(32) Poignant, F.; Freysz, J. L.; Daturi, M.; Saussey, J. *Catal. Today* **2001**, *70*, 197.
(33) Iwasaki, M.; Shinjoh, H. *Phys. Chem. Chem. Phys.* **2010**, *12*, 2365.
(34) Martins, G. V. A.; Berlier, G.; Bisio, C.; Coluccia, S.; Pastore, H. O.; Marchese, L. *J. Phys. Chem. C* **2008**, *112*, 7193.
(35) Brandenberger, S.; Krocher, O.; Wokaun, A.; Tissler, A.; Althoff, R. *J. Catal.* **2009**, *268*, 297.
(36) Schwidder, M.; Kumar, M. S.; Bentrup, U.; Perez-Ramirez, J.; Brueckner, A.; Gruenert, W. *Microporous Mesoporous Mater.* **2008**, *111*, 124.
(37) Bevilacqua, M.; Montanari, T.; Finocchio, E.; Busca, G. *Catal. Today* **2006**, *116*, 132.
(38) Klukowski, D.; Balle, P.; Geiger, B.; Wagloehner, S.; Kureti, S.; Kimmerle, B.; Baiker, A.; Grunwaldt, J. D. *Appl. Catal., B* **2009**, *93*, 185.
(39) Dedecek, J.; Capek, L.; Sazama, P.; Sobalik, Z.; Wichterlova, B. *Appl. Catal., A* **2011**, *391*, 244.
(40) Suzuki, K.; Noda, T.; Katada, N.; Niwa, M. *J. Catal.* **2007**, *250*, 151.
(41) Luo, J.-Y.; Oh, H.; Henry, C.; Epling, W. *Appl. Catal., B* **2012**, *123−124*, 296.
(42) Onida, B.; Gabelica, Z.; Lourenco, J.; Garrone, E. *J. Phys. Chem.* **1996**, *100*, 11072.
(43) Akah, A. C.; Nkeng, G.; Garforth, A. A. *Appl. Catal., B* **2007**, *74*, 34.
(44) Delahay, G.; Valade, D.; Guzman-Vargas, A.; Coq, B. *Appl. Catal., B* **2005**, *55*, 149.
(45) Nova, I.; Ciardelli, C.; Tronconi, E.; Chatterjee, D.; Bandl-Konrad, B. *Catal. Today* **2006**, *114*, 3.
(46) Malpartida, I.; Marie, O.; Bazin, P.; Daturi, M.; Jeandel, X. *Appl. Catal., B* **2012**, *113*, 52.
(47) Grossale, A.; Nova, I.; Tronconi, E. *J. Catal.* **2009**, *265*, 141.
(48) Sun, Q.; Gao, Z. X.; Chen, H. Y.; Sachtler, W. M. H. *J. Catal.* **2001**, *201*, 89.
(49) Szanyi, J.; Kwak, J. H.; Moline, R. A.; Peden, C. H. F. *Phys. Chem. Chem. Phys.* **2003**, *5*, 4045.
(50) Iwasaki, M.; Shinjoh, H. *Phys. Chem. Chem. Phys.* **2010**, *12*, 2365.
(51) Desikusumastuti, A.; Staudt, T.; Happel, M.; Laurin, M.; Libuda, J. *J. Catal.* **2008**, *260*, 315.
(52) Deka, U.; Juhin, A.; Eilertsen, E. A.; Emerich, H.; Green, M. A.; Korhonen, S. T.; Weckhuysen, B. M.; Beale, A. M. *J. Phys. Chem. C* **2012**, *116*, 4809.
(53) Deka, U.; Lezcano-Gonzalez, I.; Weckhuysen, B. M.; Beale, A. M. *ACS Catal.* **2013**, *3*, 413.
(54) Ahrens, M.; Marie, O.; Bazin, P.; Daturi, M. *J. Catal.* **2010**, *271*, 1.
(55) Ciardelli, C.; Nova, I.; Tronconi, E.; Chatterjee, D.; Bandl-Konrad, B.; Weibel, M.; Krutzsch, B. *Appl. Catal., B* **2007**, *70*, 80.
(56) Yeom, Y. H.; Henao, J.; Li, M. J.; Sachtler, W. M. H.; Weitz, E. *J. Catal.* **2005**, *231*, 181.
(57) Ciardelli, C.; Nova, I.; Tronconi, E.; Chatterjee, D.; Bandl-Konrad, B. *Chem. Commun.* **2004**, *23*, 2718.
(58) Li, M. J.; Henao, J.; Yeom, Y.; Weitz, E.; Sachtler, W. M. H. *Catal. Lett.* **2004**, *98*, 5.
(59) Nova, I.; Ciardelli, C.; Tronconi, E.; Chatterjee, D.; Bandl-Konrad, B. *Catal. Today* **2006**, *114*, 3.
(60) Chen, H. Y.; Sun, Q.; Wen, B.; Yeom, Y. H.; Weitz, E.; Sachtler, W. M. H. *Catal. Today* **2004**, *96*, 1.
(61) Savara, A.; Li, M.-J.; Sachtler, W. M. H.; Weitz, E. *Appl. Catal., B* **2008**, *81*, 251.
(62) Forzatti, P.; Nova, I.; Tronconi, E. *Angew. Chem., Int. Ed.* **2009**, *48*, 8366.
(63) Forzatti, P.; Nova, I.; Tronconi, E. *Ind. Eng. Chem. Res.* **2010**, *49*, 10386.
(64) Grossale, A.; Nova, I.; Tronconi, E. *Catal. Lett.* **2009**, *130*, 525.